JACC Vol. 33, No. 1
January 1999:267–72

Effect of Congestive Heart Failure on In Vivo Canine Aortic Elastic Properties

ZIA KHAN, MD,* RONALD W. MILLARD, PHD,† MARJORIE GABEL,*
RICHARD A. WALSH, MD, FACC,* BRIAN D. HOIT, MD, FACC*
Cincinnati, Ohio

Objectives. **The aim of this study was to characterize fully in vivo aortic compliance over a wide range of passive distending pressures, and to study pharmacologically induced alterations in compliance using an intravascular ultrasound–based technique in the canine model of heart failure.**

Background. **Altered aortic compliance may influence considerably the function of the failing heart. Although some studies demonstrate that patients with heart failure have decreased aortic compliance, data from other studies are conflicting.**

Methods. **Aortic pressures and dimensions in seven dogs were determined both before and after pacing-induced congestive heart failure (CHF) using simultaneous micromanometer and intravascular ultrasound transducers. Decreases in aortic pressure were produced at baseline and after nitroprusside and dobutamine infusions. Inner and outer aortic circumferences were drawn at the lumen–intimal and media–adventitial borders.**

Results. **Aortic pressure–dimension (chamber) stiffness constants were greater after heart failure was produced (10.0 ± 1.5 vs. 6.7 ± 1.5, $p < 0.05$), but stress–strain stiffness (material) constants were similar (11.4 ± 1.8 vs. 11.3 ± 1.0, p = NS). Equivasodilating doses of nitroprusside and 10 μg/kg/min dobutamine decreased pressure–dimension stiffness constants after pacing-induced heart failure but not beforehand. The aortic wall thickness to diameter ratio was significantly greater in CHF than in the control condition (0.30 ± 0.08 vs. 0.16 ± 0.03, $p < 0.01$).**

Conclusions. **Aortic compliance is decreased in this model of CHF, and this change is attributable primarily to vessel geometry rather than material properties. Equivasodilating doses of nitroprusside and equivalent doses of dobutamine increase aortic chamber compliance in dogs with CHF, but not in normal dogs. These data suggest that the beneficial effects of nitroprusside and dobutamine in CHF occur in part from improvement in aortic compliance.**

(J Am Coll Cardiol 1999;33:267–72)

The input impedance of the arterial system is an important determinant of the stroke work and power output of the left ventricle (1–3) and is comprised of systemic vascular resistance, total arterial compliance and wave reflections (4). A decrease in aortic compliance (i.e., increase in stiffness) represents an increase in the opposition to left ventricular ejection, and therefore is a component of the ventricular afterload (5); as such, altered aortic compliance may influence considerably the function of the failing heart. Although some studies demonstrate that patients with heart failure (6,7) have decreased aortic compliance, data from other studies are conflicting (8,9).

Various models have been used to assess the elastic behavior and compliance of the aorta. In vitro studies employ either segments, rings or helical strips cut from blood vessels and measure force–length relations and wall thickness (10). These methods are limited by the inability to extrapolate to the intact circulation and because isolated aortic specimens are difficult to maintain. Early investigations of arterial elasticity in vivo attached instruments to blood vessels in situ (11); however, these techniques impose mechanical constraints on the vessel, and are therefore undesirable. More recently aortic distensibility and pressure–dimension relations of the aorta have been accomplished with transcutaneous and intravascular ultrasound (12–14).

Accordingly, the aim of this study was to characterize fully in vivo aortic compliance over a wide range of passive distending pressures, and to study pharmacologically induced alterations in compliance using an intravascular ultrasound (IVUS)-based technique in the canine model of heart failure (15). Specifically, we tested the hypothesis that compliance in the abdominal aorta is decreased in dogs with pacing-induced heart failure owing to altered aortic geometry and that compliance can be pharmacologically modulated.

Methods

The experimental protocol was approved by the Institutional Animal Care and Use Committee at the University of Cincinnati.

From the *Division of Cardiology, Department of Internal Medicine and †Department of Pharmacology and Cell Biophysics, University of Cincinnati, Cincinnati, Ohio. Sponsored in part by an American Heart Association Fellowship Award SW-95-27F and American Heart Association Grant-in-Aid, Ohio Affiliate SW-96-14-S and The Ohio Board of Regents Investment Fund for Cardiovascular Biomaterials.

Manuscript received May 20, 1998; revised manuscript received August 3, 1998, accepted September 15, 1998.

Address for correspondence: Brian D. Hoit, MD, Division of Cardiology, University of Cincinnati, P.O. Box 670542, Cincinnati, Ohio 45267-0542.

0735-1097/99/$20.00
PII S0735-1097(98)00530-0

Abbreviations and Acronyms

IVUS = intravascular ultrasound
k_{pd} = stiffness constant of the pressure–dimension relation
k_{ss} = stiffness constant of the stress–strain relation
SVR = systemic vascular resistance

Seven adult mongrel conditioned dogs, weighing 22.2 ± 3.2 kg, were used for this study. Animals were anesthetized with pentobarbital (30 mg/kg/IV), intubated and ventilated. A unipolar pacemaker lead was passed via the right internal jugular vein into the right ventricular apex, and a pulse generator (Medtronic Spectrax) was implanted in the subcutaneous tissue over the back of the neck. Rapid ventricular pacing at 250 bpm for 3–4 weeks was used to produce low output heart failure (15).

Instrumentation. At the time of study, animals were placed on a fluoroscopy table, anesthetized with pentobarbital (30 mg/kg/IV), intubated and ventilated. A table warmer was used to ensure normothermia. Under fluoroscopic guidance, a 7-F Fogarty catheter was advanced into the descending aorta via the carotid artery to a level just above the 12th rib. An 8-F triple lumen thermodilution catheter was advanced into the pulmonary artery via the jugular vein. The femoral arteries were secured by cutdowns through which a 5-F Millar micromanometer and a 6.2-F IVUS catheter with a 12-MHz ultrasound transducer (Sonocath CV, Mansfield) were advanced through a 10-F sheath into the descending aorta to the level of the 12th rib. The micromanometer was gradually withdrawn until its catheter artifact was no longer evident in the IVUS image.

Experimental protocol. Hemodynamic and echocardiographic studies were performed both before and after production of pacing-induced heart failure. Ganglionic blockade with hexamethonium bromide (45 mg/kg/IV) was used to avoid the confounding influence of autonomic reflexes, and animals were paced to achieve constant heart rates before and after heart failure. The aorta was "preconditioned" to minimize viscoelastic effects (hysteresis, creep and stress relaxation) by four to five brief aortic occlusions (16).

Hemodynamic and IVUS data were obtained at baseline. After baseline data were acquired, the aortic balloon was inflated in graded steps to acquire several (at least five) steady-state runs representing a range of aortic distending pressures from baseline to the mean circulatory pressure (~25 mm Hg). The protocol was repeated after randomly assigned infusions of both the directly acting vasodilator sodium nitroprusside (40 to 120 g/min to achieve a 20% decrease in aortic systolic pressure) and the beta-agonist, dobutamine, at a fixed dose of 10 μg/kg/min. Thermodilution cardiac outputs were determined in triplicate and averaged at baseline and after each pharmacologic intervention.

One animal underwent pacemaker lead implantation without rapid pacing and was used as a sham-operated time control.

Data acquisition. Intravascular ultrasound studies were recorded on a Hewlett-Packard Sonos 100 intravascular imaging system. Ultrasound images were recorded continuously on one half–inch S-VHS videotape.

The micromanometer and fluid-filled catheters were calibrated before implantation with a mercury manometer. Zero drift of the micromanometer was corrected by matching the aortic pressure measured simultaneously through the fluid-filled lumen. Fluid-filled catheters were connected to 23-dB transducers with zero pressure at the level of the mid right atrium. Analog signals for the high fidelity and fluid-filled aortic pressures, pulmonary arterial and right atrial pressures and the electrocardiogram were recorded on-line on a Gould multichannel recorder and digitized every 2 ms through an analog-to-digital board (Dual Control Systems) interfaced to a Comp-U-Dyne 486 DX and stored on floppy disk. Data were acquired over 5 s with respiration suspended at end inspiration. The electrocardiogram was recorded simultaneously via the auxiliary channel of the ultrasonograph. A synchronizing event marker was registered on both the ultrasonograph and the Gould recorder.

Data analysis. Cross-sectional video images of the aorta were analyzed off-line on a dedicated image analysis system (Tomtec). Images were replayed by using a videocassette recorder with high quality still/slow capability and viewed on a high resolution video monitor.

The internal vessel circumferences were measured by tracing the acoustic interface between the lumen and the intimal leading edge, and the external circumference was measured by tracing the acoustic interface between the medial–adventitial border. Preocclusion data were analyzed at both maximum (end systole) and minimum aortic dimension; steady-state measurements during occlusion were made at maximum dimension only. Measurements were made from three cycles and were averaged. Internal and external vessel diameter were calculated from their respective circumferences:

$$D = \text{circumference}/\pi.$$

Curve fitting and calculation of elastic properties. Aortic systolic and maximum internal vessel diameters were fit to a simple monoexponential equation:

$$P = Ae^{K_{pd}D},$$

where valve P is the aortic systolic pressure, D is the corresponding maximal internal vessel diameter, A is the pressure intercept, e is the base of the natural logarithm, and K_{pd} is the chamber stiffness constant.

Stress was calculated using the law of Laplace:

$$\text{Stress} = P \times D/2h,$$

where h = aortic wall thickness.

Strain was computed as a natural strain:

$$\text{strain} = \ln (D/D_{min}),$$

where D_{min} is the diameter at mean circulatory pressure (aortic balloon completely inflated).

Table 1. Hemodynamic Changes With Intervention

	Baseline			Nitroprusside			Dobutamine		
	HR (bpm)	BP (mm Hg)	SVR (dyn·s·cm^{-5})	HR (bpm)	BP (mm Hg)	SVR (dyn·s·cm^{-5})	HR (bpm)	BP (mm Hg)	SVR (dyn·s·cm^{-5})
CON	121 ± 15	143 ± 16	2,170 ± 331	144 ± 10*	117 ± 22*	1,727 ± 408*	144 ± 6*	195 ± 52*†	2,110 ± 783
PHF	130 ± 14	117 ± 12‡	2,929 ± 403‡	146 ± 8*	98 ± 13	2,275 ± 362*‡	149 ± 9*	119 ± 16‡	2,384 ± 425*

*$p < 0.05$ vs. baseline. †$p < 0.05$ vs. nitroprusside. ‡$p < 0.05$ vs. control. n = 7. BP = systolic arterial blood pressure; CON = control; HR = heart rate; PHF = pacing-induced heart failure; SVR = systemic vascular resistance.

Stress–strain data were also fitted to a simple monoexponential equation:

$$\sigma = Ae^{k_{ss}\varepsilon},$$

where σ = stress, ε = strain and k_{ss} is the material stiffness constant. Pressure–dimension and stress–strain data were measured from aortic occlusions taken at baseline and during nitroprusside and dobutamine; measurements were made both before and after heart failure was produced.

Interpretative variability. Measurement variability for aortic circumferences were assessed by measuring randomly selected intravascular ultrasound images (n = 20) for two blinded observers. Differences were calculated as the difference between two observations divided by the mean of the two observations, and expressed as a percent.

Statistics. Group data are expressed as mean ± SD. Two-way repeated measures analysis of variance was used to test the effects of pharmacologic agents and heart failure; when a significant interaction was present, differences were tested with contrasts. Paired *t* tests were used to compare parameters in the control and heart failure groups. Differences were considered significant at a value of $p < 0.05$.

Results

The percent interobserver difference for luminal–intimal and medial–adventitial border measurements (n = 49 beats) were 7.0 ± 3.4% and 5.8 ± 3.2%, respectively.

Comparison of control and heart failure data at baseline. The systemic arterial pressure was significantly lower and the systemic vascular resistance was significantly greater in dogs after production of congestive heart failure than obtained in the same animal before heart failure (Table 1).

Nitroprusside produced a 20.4% fall in systemic vascular resistance (SVR) in the control state and a 22.3% decrease in SVR after heart failure was produced (both $p < 0.05$). In contrast, dobutamine produced a change in SVR only in the dogs with heart failure.

Cardiac output was significantly greater in the control than heart failure state (3.8 ± 1.1 vs. 2.3 ± 3.5 liters/min, $p < 0.01$) and increased in response to both nitroprusside and dobutamine ($p < 0.001$).

The aortic diameter decreased and wall thickness increased in heart failure compared to control dogs. As a result, the wall thickness to diameter ratio was significantly greater in heart failure than control dogs (Table 2).

Effect of heart failure and pharmacologic agents on aortic pressure–diameter relationships. Pressure–diameter curves from a representative animal are shown in Figure 1, and the mean chamber stiffness constants (k_{pd}) before and after production of heart failure are shown in Table 3. The k_{pd} was significantly greater after heart failure was produced than before, indicating decreased aortic compliance owing to pacing-induced heart failure. There was no significant effect of either nitroprusside or dobutamine on the k_{pd} in the control state. In contrast, nitroprusside and dobutamine significantly reduced k_{pd} and shifted the pressure–dimension relation significantly to the right with heart failure. However, the pressure–dimension relation did not return to that observed in the control state.

Effects of heart failure and pharmacologic agents on aortic stress–strain relationships. Stress–strain curves from a representative animal are shown in Figure 2, and mean aortic material stiffness constants are shown in Table 3. The stiffness constant of the stress–strain relation, k_{ss}, was unaffected by pacing-induced heart failure. Moreover, the stiffness constant was not altered by nitroprusside and dobutamine either before or after production of heart failure.

No changes were observed in the sham-operated time control dog.

Discussion

The present study examined aortic mechanics over a wide range of systolic aortic pressures using intravascular ultrasound and high fidelity pressure measurements and graded balloon occlusion of the aorta in the normal and heart failure canine model in vivo. The principal finding of this study is that aortic compliance is decreased in pacing-induced heart failure, and the reduced aortic compliance in heart failure returns toward normal with the use of the vasodilator nitroprusside and the inotropic agent dobutamine.

Table 2. Changes in Aortic Diameter and Wall Thickness in Pacing-Induced Heart Failure (PHF)

	Baseline Diameter (D, cm)	Baseline Thickness (h, cm)	h/D
Control	0.92 ± 0.11	0.15 ± 0.03	0.16 ± 0.03
PHF	0.73 ± 0.08*	0.22 ± 0.05*	0.30 ± 0.08*

*$p < 0.05$ vs. control.

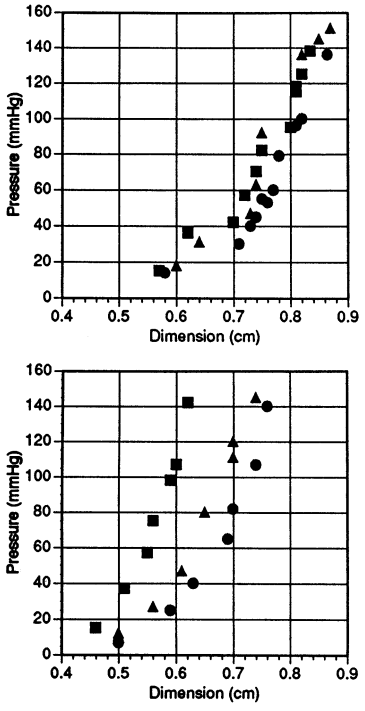

Figure 1. Representative pressure–dimension curves before **(top)** and after **(bottom)** pacing-induced heart failure in the baseline state **(squares)** and after nitroprusside **(circles)** and dobutamine **(triangles).** A shift of the pressure–dimension relation with nitroprusside and dobutamine occurred only after heart failure was produced.

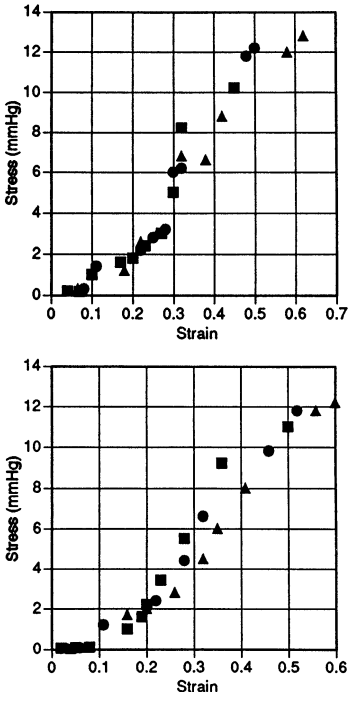

Figure 2. Stress–strain curves before **(top)** and after **(bottom)** pacing-induced heart failure in the baseline state **(squares)** and after nitroprusside **(circles)** and dobutamine **(triangles).** Stress–strain relations were similar in both states.

Aortic compliance in heart failure. The mechanisms responsible for altered aortic compliance in congestive heart failure are incompletely understood and include alterations of the vascular wall (i.e., collagen, elastin, vascular smooth muscle) changes in vessel geometry (remodeling) and neurohormonal influences. We showed that congestive heart failure is associated with increased wall thickness, both in absolute terms and relative to the luminal diameter. An important finding is that change in aortic compliance in pacing-induced heart failure is attributable largely to geometric factors, rather than to material properties of the vessel, since the stiffness constant of the stress–strain relation (which accounts for vessel geometry and reflects changes in material properties) was unchanged after heart failure was produced. Another possible mechanism for vessel remodeling and the resultant decreased aortic compliance in heart failure is sodium retention within the vessel wall. Administration of mineralocorticoids to induce salt retention has been shown to increase vascular stiffness (17). Although a potential explanation is that operative compliance is decreased secondary to an overdistended aorta operating on a steeper portion of its pressure–diameter relationship, this is unlikely, since aortic diameters were lower in the animals with heart failure compared to control animals.

The structural basis for changes in aortic compliance is better characterized for aging and hypertension than for heart failure. Reduced aortic compliance in hypertension is associated with increased arterial wall thickness and changes in the structural composition of the arterial wall (18). There is evidence that the elevated arterial pressure is not the only determinant of medial hypertrophy (19). Angiotensin II has been implicated in the adaptive vascular changes during hypertension; studies have shown that angiotensin II exerts a hypertrophic effect and induces polyploidy in vascular smooth muscle cells (4), and that local vascular renin angiotensin systems exist (20). There is also evidence that long-term angiotensin-converting enzyme inhibition may normalize arterial stiffness and vascular architecture in hypertensive rats (18).

Table 3. Pressure–Dimension and Stress–Strain Relations: Effects of Pacing-Induced Heart Failure (PHF) and Pharmacologic Agents

	Pressure–Dimension (mm Hg/cm)			Stress–Strain (mm Hg)		
	Baseline	Nitroprusside	Dobutamine	Baseline	Nitroprusside	Dobutamine
Control	6.7 ± 1.5	6.9 ± 1.3	6.9 ± 1.8	11.3 ± 1.0	11.3 ± 2.9	11.6 ± 1.9
PHF	10.0 ± 2.3*	8.3 ± 1.9*†	8.3 ± 1.8*†	11.4 ± 1.8	11.7 ± 1.2	12.5 ± 1.2

*$p < 0.05$ vs. control. †$p < 0.05$ vs. baseline.

Effect of drugs on arterial compliance. The resting caliber of the aorta depends on the balance between passive (pressure-induced) expansion and active contraction (16). Pressure dependence of arterial caliber is evident in that a fall of blood pressure from 143 ± 16 mm Hg to 21 ± 9 mm Hg (all baseline runs) produced a 39% decrease in diameter. Smooth muscle relaxation produced by nitroprusside increased aortic compliance significantly in the heart failure dogs, although not quite to the levels observed in normal control dogs; that is, the aorta remained stiffer than the aorta in control animals under a similar degree of vasodilation. Nevertheless, our results are similar to those of Pepine et al., who showed that nitroprusside increased aortic compliance in patients with congestive heart failure (21).

There are four competing factors that determine the effect of a vasoactive drug on aortic compliance. First is the direct effect of the drug on the aortic wall smooth muscle. The active tension that the smooth muscle can generate is estimated between 1.5 and 2.5 $\times$ 10^5 dyn/cm^2 (4); the loss of this tension as a result of smooth muscle relaxation should increase vessel compliance. Second, a vasoactive drug may alter aortic diameter. If an artery exhibits the same change in radius for a given change in pressure in both the vasodilated and vasoconstricted state, then the former will be more compliant than the latter because of geometric considerations. Third, the arterial size resulting from a vasoactive agent may influence the fractional recruitment of collagen. The relation between pressure and diameter (or stress and strain) in a blood vessel is curvilinear and concave toward the pressure or stress axis. This is partly a result of differential loading of the distensible elastin and relatively stiff collagen at different pressure (stress) or diameter (strain) (22,23). As smooth muscle is relaxed and arterial caliber increases, one would expect the fractional recruitment of collagen to increase and the vessel to become less compliant. The final factor relates to the interaction or linking between collagen, elastin and smooth muscle within the arterial wall. Although a number of models have been proposed for the arrangement (series and parallel) (24), there is as yet no general agreement on a model that fits all the experimental data. Several investigators have proposed that smooth muscle in the arterial wall functions in series with collagen, and both operate in parallel with elastin (22). During smooth muscle contraction the collagen jacket is tensed, making the vessel stiffer, and with smooth muscle relaxation stress is released from collagen and transferred to the more distensible elastin. The data from our study of heart failure animals is in agreement with this model. If the slopes of the pressure–area curves are examined at equivalent diameters (Fig. 2), it is apparent that the vasodilated vessel is markedly more compliant than at baseline.

Dobutamine also decreased aortic stiffness in dogs with heart failure. This finding is consistent with results from a previous heart failure study in which therapy with dobutamine produced beneficial changes in the aortic impedance spectrum, that is, impedance matching and facilitation of ventricular vascular coupling (6).

The effects of vasodilation on aortic compliance are not apparent in dogs without heart failure and contrast with other studies (25,26). One possible explanation is that the arteries studied in these cases were all muscular arteries; the effects of drugs on arterial caliber in muscular arteries is likely to be greater than those on elastic arteries such as the aorta. This assumption is consistent with the hypothesis that vascular smooth muscle hypertrophy in the aorta of heart failure animals is responsible for the altered compliance and vasoreactivity.

Methodological considerations. A number of potential limitations merit comment. First, an important issue regarding the techniques used to assess aortic elastic mechanics is the precision and reproducibility of aortic circumference and wall thickness measurements. Intravascular ultrasound measurements have been shown in a number of studies to correlate well with angiographic and pathologic assessments of arterial luminal dimensions and wall thickness (27–29). Nevertheless, the method has potential limitations including artifacts owing to catheter tilt and blood and wall echo signal attenuation. Second, the elastic parameters measured with this technique were obtained from a wide range of pressures generated by graded balloon occlusion of the aorta. The potential of viscous and inertial behavior influencing the purely elastic behavior of the aorta cannot be entirely ruled out. However, prior to each experiment "preconditioning" of the aorta was done by repeated graded inflation and deflation of the balloon. Third, our method of aortic pressure alteration may itself produce reflex changes in the determinants of aortic compliance. Reflex alterations were minimized in our protocol by employing ganglionic blockade. Moreover, the aortic balloon was inflated sufficiently proximal to the catheters so as not to directly interfere with pressure–diameter measurements. Finally, despite the mechanistic insights, careful histologic and molecular biologic analysis of the arterial wall are necessary to completely understand the findings in our study.

Clinical implications. The pathophysiologic and therapeutic implications of these findings are considerable. Structural changes in the conduit arteries are maladaptive in that they increase left ventricular afterload and reduce left ventricular pump efficiency. We have shown that vasodilators have differential effects on resistance and conduit vessels. It is interesting to speculate that the beneficial effects of angiotensin-converting enzyme inhibitors in heart failure are due, in part, to large vessel remodeling with resultant increased compliance. The framework established in this study may be used for the development of pharmacologic therapies that specifically affect aortic compliance and favorably influence ventricular–arterial coupling and hydraulic efficiency of the left ventricle.

Conclusions. An intravascular technique for measurement of aortic elastic properties in the normal and heart failure canine model in vivo has been described. We conclude that 1) aortic compliance is decreased in the rapid pacing model of congestive heart failure; 2) this change is attributable primarily to vessel geometry rather than material properties, and 3) equivasodilating doses of nitroprusside and equivalent doses of

dobutamine increase aortic compliance in dogs with congestive heart failure, but not in the normal dogs.

We acknowledge the expert secretarial assistance of Norma Burns.

References

1. Elzinga G, Westerhof N. Pressure and flow generated by the left ventricle against different impedances. Circ Res 1973;32:178–86.
2. Maughan WL, Sunagawa K, Burkhoff D, Sagawa K. Effect of arterial impedance changes on the end-systolic pressure volume relation. Circ Res 1984;54:595–602.
3. Milnor WR. Arterial impedance as ventricular afterload. Circ Res 1975;36: 565–70.
4. Nichols WW, O'Rourke MF. Properties of the arterial wall. In: Nichols WW, O'Rourke MF, editors. McDonald's Blood Flow in Arteries. London: Edward Arnold, 1990:77–124.
5. Simon AC, O'Rourke MF, Levenson J. Arterial distensibility and its effects on wave reflection and cardiac loading in cardiovascular disease. Coron Artery Dis 1991;2:1111–20.
6. Binkley PF, Van Fossen DB, Nunziata E, Unverferth DV, Leier CV. Influence of positive inotropic therapy on pulsatile hydraulic load and ventricular-vascular coupling in congestive heart failure. J Am Coll Cardiol 1990;15:1127–35.
7. Pepine CJ, Nichols WW, Conti CR. Aortic input impedance in heart failure. Circulation 1978;58:460–5.
8. Laskey WK, Kussmaul WG, Martin JL, Kleveland JP, Hirshfeld JR Jr, Schroff S. Characteristics of vascular hydraulic load in patients with heart failure. Circulation 1985;72:61–71.
9. Merillon JP, Fonteiner G, Lerallut JF, et al. Aortic input impedance in heart failure: comparison with normal subjects and its changes during vasodilator therapy. Eur Heart J 1984;5:447–55.
10. Cox RH. Comparison of arterial wall mechanics using ring and cylindrical segments. Am J Physiol 1983;244:H298–303.
11. Peterson LH, Jensen RE, Parnell J. Mechanical properties of arteries *in vivo*. Circ Res 1960;8:622–39.
12. Bank AJ, Wang H, Holte JE, Mullen K, Shammas R, Kubo SH. Contribution of collagen, elastin, and smooth muscle to *in vivo* human brachial artery wall stress and elastic modulus. Circulation 1996;94:3263–70.
13. Stefanadis C, Stratos C, Vlachopoulos C, et al. Pressure-diameter relation of the human aorta: a new method of determination by the application of a special ultrasonic dimension catheter. Circulation 1995;92:2210–9.
14. Tawakol A, Omland T, Gerhard M, Wu JT, Creager MA. Hyperhomocyst (e) inemia is associated with impaired endothelium-dependent vasodilation in humans. Circulation 1997;95:1119–21.
15. Hoit BD, Shao Y, Gabel M, Walsh RA. Left atrial mechanical and biochemical adaptation to pacing-induced cardiomyopathic heart failure. Cardiovasc Res 1995;29:469–74.
16. Gow BS. Circulatory correlates: vascular impedance, resistance and capacity. In: Geiger SR, et al. Handbook of Physiology, Section 2, The Cardiovascular System. Vol 2. Baltimore: American Physiological Society, 1980:353–408.
17. Zelis R, Mason T. Diminished forearm arteriolary dilator capacity produced by mineralocorticoid-induced salt retention in man: implications concerning congestive heart failure and vascular stiffness. Circulation 1970;41:589–92.
18. Levy BI, Michael JB, Salzmann JL, et al. Effects of chronic inhibition of converting enzyme on mechanical and structural properties of arteries in rat renovascular hypertension. Circ Res 1988;63:227–39.
19. Owens GK. Influence of blood pressure on development of aortic medial smooth muscle hypertrophy in spontaneously hypertensive rats. Hypertension 1987;9:178–87.
20. Hirsch AT, Talsness CE, Schunkert H, Paul M, Dzau VJ. Tissue-specific activation of cardiac angiotensin converting enzyme in experimental heart failure. Circ Res 1991;69:475–82.
21. Pepine CJ, Nichol WW, Curry RC, Conti CR. Aortic input impedance during nitroprusside infusion. J Clin Invest 1979;64:643–54.
22. Burton AC. Relation of structure to function of the tissues of the wall of blood vessels. Physiol Rev 1954;34:619–42.
23. Roach MR, Burton AC. The reason for the shape of the distensibility curves of arteries. Can J Biochem Physiol 1957;35:681–90.
24. Dobrin P, Canfield T. Identification of smooth muscle series elastic component in intact carotid artery. Am J Physiol 1977;232:H122–30.
25. Bank AJ, Wilson RF, Kubo SH, Holte JE, Dresing TJ, Wang H. Direct effects of smooth muscle relaxation and contraction on *in vivo* human brachial artery elastic properties. Circ Res 1995;77:1008–16.
26. Westling H, Jansson L, Jonson B, Nilsen R. Vasoactive drugs and elastic properties of human arteries *in vivo*, with special reference to the action of nitroglycerine. Eur Heart J 1984;5:609–16.
27. Gussenhoven WJ, Essed CE, Lancee C, et al. Arterial wall characteristic determined by intravascular ultrasound imaging: an *in vitro* study. J Am Coll Cardiol 1989;14:947–52.
28. Nishimura RA, Edwards WD, Warnes CA, et al. Intravascular ultrasound imaging: *in vitro* validation and pathologic correlation. J Am Coll Cardiol 1990;16:145–54.
29. Nissen SE, Grines CL, Gurley JC, et al. Application of a new phased-array ultrasound imaging catheter in the assessment of vessel dimensions: *in vivo* comparison to cineangiography. Circulation 1990;81:660–6.